BOSTON UNIVERSITY

GRADUATE SCHOOL OF ARTS AND SCIENCES

Thesis

THE EFFECT OF EVAPORATION AND NUTRIENT ENRICHMENT ON THE ERODABILITY OF MUDFLATS IN A MESOTIDAL ESTUARY

by

TAMMY LYNN VIGGATO

B.S., Illinois Wesleyan University, 2004

Submitted in partial fulfillment of the

requirements for the degree of

Master of Science

2013

Approved by

First Reader   _____

Sergio Fagherazzi, Ph.D.
Associate Professor of Earth and Environment

Second Reader   _____

Robinson Fulweiler, Ph.D.
Assistant Professor of Earth and Environment
Assistant Professor of Biology

Third Reader   _____

Guido Salvucci, Ph.D.
Professor of Earth and Environment

ACKNOWLEDGMENTS

THE EFFECT OF EVAPORATION AND NUTRIENT ENRICHMENT ON THE ERODABILITY OF MUDFLATS IN A MESOTIDAL ESTUARY

TAMMY VIGGATO

ABSTRACT

Large areas of mesotidal estuaries become subaerial during low tide. Here we study the effect of nutrient enrichment and several meteorological and hydrodynamic parameters on the erodability of mudflat substrates when they are emergent. Results from high resolution measurements in Plum Island Sound, Massachusetts, USA indicate that daily nutrient enrichment at 70 µM NO3− does not change the critical shear stress of the muddy substrate, nor affect the concentration of Chlorophyll *a* at the surface. Sediment erodability is instead directly related to the potential evaporation rate and to the duration of the subaerial period. Chlorophyll *a* concentration decreases when evaporation is high, possibly due to the downward migration of diatoms. Sediment concentrations in the water column during submergence strongly depend on bottom shear stresses triggered by tidal currents. Surprisingly, they are also related to the total evaporation that occurred in the previous emergence period. We conclude that subaerial desiccation at low tide decreases the erodability of mudflat sediments. This strengthening effect is not lost during the following submerged period, thus limiting the erosive effect of tidal currents. For the first time we therefore show that not only subaqueous but also subaerial processes control the erodability of mudflats. Global warming and other climatic variations regulating long-term evaporation rates can therefore directly affect the stability of mudflats in mesotidal environments.

TABLE OF CONTENTS

LIST OF TABLES

LIST OF FIGURES

LIST OF ABBREVIATIONS

ADV   Acoustic Doppler Velocimeter

CSM   Cohesive Strength Meter

LTER   Long Term Ecological Research site

MBL   Marine Biological Laboratory

MPB   Microphytobenthos

**do I need to list all of the equation variables?

Introduction

Mudflats are an important component of the coastal landscape: they protect coastal communities from flooding and storm surges (Scavia 2002, Meire 2005), maintain water quality through nutrient cycling and pollutant filtration (Van Damme et al 2005), and provide a critical foraging habitat for birds and fish (Little 2000, Galbraith et al 2002).

Meteorological and tidal conditions affect sediment erosion and deposition in mudflats, the geotechnical properties of the substrate, as well as biological variability and productivity (Amos 1987). Anthropogenic stressors such as coastal eutrophication and climate change could alter the biological and physical equilibrium of mudflats (Galbraith et al 2002, Meire 2005). For example, an increase in the frequency of storms combined with sea level rise could significantly impact the erosion rates and overall morphology of these landforms (Mariotti et al 2010). A thorough understanding of sediment stability in mudflats is necessary for the preservation of these delicate environments.

Critical shear stress, the magnitude of shear stress sediments may withstand before significant erosion occurs, is a key parameter controlling erosion of tidal flats (Anderson, 2007). Tidal flat sediments are subject to varying shear stresses over tidal cycles due to water currents (Fagherazzi and Mariotti 2012) and propagation of wind waves (Mariotti and Fagherazzi 2012). Sediments with higher critical shear stress are less susceptible to erosion and therefore are able to withstand higher levels of shear stress before sediment resuspension occurs.

Numerous studies have shown that the critical shear stress of cohesive sediments in muddy tidal flats is controlled by a complex combination of physical, chemical and

biological factors (e.g. Black et al, 2002, Defew et al 2002, 2003). Site-specific

properties, such as sediment characteristics (density, organic content, grain size) as well

as the presence or absence of macro fauna, submerged vegetation, and biofilms make the

key processes responsible for sediment stability hard to discern (Defew et al, 2002).

Mudflats are often colonized by biofilms, of which microphytobenthos (a

photosynthetic diatom-dominated assemblage of unicellular, eukaryotic organisms) is a

major component (MacIntyre et al. 1996). Among other factors, microphytobenthos

growth is susceptible to light, temperature, and nutrient availability, leading to seasonal

changes in their abundance (Davoult, 2009). Microphytobenthos produce an extracellular

carbohydrate matrix that may contribute to sediment stabilization (e.g. de Brouwer et al

2002, Tolhurst et al 2003, deBrouwer et al. 2005). Previous research has found a positive

correlation between biofilm biomass and critical shear stress in tidal flat sediments (e.g.

Underwood and Paterson, 1993, Black et al, 2002, Tolhurst et al, 2003).

The relationship between biofilm presence and increased sediment stability is thought to

be due to sediment binding and a decrease in roughness and drag on the sediment surface

(Tolhurst, 2008). The role microphytobenthos play in sediment stability may vary

throughout the tidal cycle due to their migration within the sediment (e.g. Paterson 1989,

Miller et al 1996, Defew et al 2002).

Studies of tidal mudflats have indicated that the critical shear stress varies over

emersion-immersion cycles and depends on the environmental conditions sediments are

exposed to (e.g. Amos et al. 1987, Tolhust et al 2004). Critical shear stress has been

shown to increase over tidal emersion periods, but returns to its pre-exposure value once

exposed to water from rainfall or tidal immersion (Tolhurst et al 2004). The physical properties of clay soils, which dominate tidal mudflats, can vary significantly with the degree of hydration (Hillel, 1998). The shear strength increases as the soil de-saturates and the matric soil potential increases (Zhan, 2006).

Similarly, seasonal and climatic factors have a great influence on sediment erodability when measured over long time periods (Amos et al 1987). While temporal changes in sediment critical shear stress have been studied both seasonally and over single tidal cycles, changes resulting from variations in daily environmental conditions have yet to be considered.

Here we present results on a field experiment conducted on a tidal flat in Plum Island Sound, Massachusetts in September 2011. This study explores the connections between critical shear stress, biofilm abundance, and evaporation. High-resolution field observations taken during emersion were used to identify biological and physical factors contributing to changes in critical shear stress of tidal flat sediments.

Study site

The study took place along the Rowley River Estuary in Rowley, Massachusetts (Figure 1) within the Plum Island Sound Long Term Ecological Research site. The Rowley River forms at the convergence of the Egypt River and Muddy Run in Ipswich, Massachusetts and covers a drainage area of 9.6 square miles (Commonwealth of Massachusetts, 1999; Commonwealth of Massachusetts, 2003). The Rowley River flows into Plum Island Sound, a semi-diurnal estuary connected to the Gulf of Maine that experiences a mean tidal range of 2.6 m and spring tidal range of 3.2 m (Fagherazzi, 2012). Tidal flats

consisting of muddy sediments become exposed along the banks of the Rowley River during low tide. Previous research in this area has found that these environments support a large population of benthic, pennate diatoms (Tobias et al, 2003).

Materials and Procedures

A two-week study into the daily variability in the critical shear stress of tidal flat sediments was conducted in September 2011. High resolution field observations were used to investigate how changes in nutrient availability and environmental conditions impact the critical shear stress of tidal flat sediments during emersion. Additionally, hydrological and meteorological sensors located in proximity of the study site were used to model the hydrodynamic processes occurring during immersion. This approach was used to determine whether sediment resuspension during immersion was related to sediment erodability during the previous emersion period.

Two six meter by one meter transects were established on the mudflat stretching from the salt marsh scarp to the channel (Figure 1). The total change in elevation along each transect was less than 0.4 meters. One transect was exposed to nutrient enrichment through the direct application of liquid fertilizer (with concentration of 70 μM NO_3^-) immediately after tidal emersion each day for the duration of the project. The liquid fertilizer was applied using a lawn sprayer with the nozzle held approximately 25 cm above the sediment surface. The second transect received no fertilizer application and served as a control.

High-resolution measurements of critical shear stress, chlorophyll *a* concentration, dry density, and organic content were taken daily. Two acoustic Doppler velocimeters (ADVs) were deployed between the nutrient enriched and control transects to monitor hydrological conditions. A meteorological station located approximately 2.9 miles from the study site was used to monitor climatic conditions sediments were exposed to during tidal emersion.

A detailed description of the instruments and methods used in this research is reported below.

Critical Shear Strength

The critical shear stress of each plot was measured daily using a cohesive strength meter (CSM, Widdows, 2007, Tolhurst 1999). The CSM measures the critical shear stress of sediments by shooting a vertical jet of water with increasing force into a chamber applied on the sediment substrate. This device allows for repeated measurements taken over a shorter time period and a smaller area than other erosional devices, making it ideal for studying spatial and temporal variability within a single field site (Tolhurst, 2006). An infrared sensor monitors the turbidity levels within the chamber to determine the pressure of the jet at which significant erosion begins. The critical shear stress was determined as a change in the slope in the plot relating jet strength exerted by the CSM and turbidity measured within the chamber (Tolhurst, 1999).

Six critical shear stress measurements (three in the nutrient enriched transect and three in the control transect) were taken each day. Measurements were taken randomly within subplots, alternating between even and odd subplots daily. Critical shear stress

measurements were taken first in the fertilized plots and then in the control plots in order to maximize the number of measurements that could be taken between the exposure and submergence of the tidal flat. Each measurement took approximately 20 minutes.

Bottom velocities and shear stresses

Hydrodynamic conditions on the tidal flat were monitored by two Nortek Acoustic Doppler velocimeters (ADVs) deployed between the nutrient enriched and control transects from September 6, 2011 at 12:00 to September 29, 2011 at 00:00 (Figure 1). The first ADV (ADV1) was deployed between subplots 1 of the two transects at an elevation of -1.032 m relative to mean sea level; the second ADV (ADV2) was deployed near the marsh bank, between subplots 6 at an elevation of -0.655 m relative to mean sea level (Figure 1). The shear stress exerted on the tidal flat during each tidal cycle was calculated from the high frequency velocity measurements of the ADVs using the Reynolds stress method (Anderson, 2007).

In addition to the critical shear stress, the rate of sediment resuspension occurring over tidal cycles is critical for a complete understanding of sediment erodibility (Amos, 1992). Backscatter intensity recorded by acoustic Doppler velocimeters (ADVs) has been used herein as a proxy for suspended sediment concentration (Ha, 2009; Chanson, 2007). The backscatter signal is generated from sound pulses reflecting off particles suspended in the water column. Measuring the suspended sediment concentration with an ADV allows for water velocity and shear stress measurements to be taken in conjunction.

The maximum backscatter recorded by ADV 1 during each tidal cycle was used as an indicator of local sediment resuspension and compared to the total evaporation from the preceding emersion cycle. Backscatter for each ADV measurement is calculated as the average of the signal/noise for the x, y and z components. The maximum backscatter occurs during the flood stage of each tidal cycle, generally 1 to 1.5 hours after tidal flat immersion (Figure 2).

Emersion Periods and Variations in Bed Elevation

The ADV pressure sensors were used to determine when the tidal flat was exposed and submerged during each tidal cycle. The time of exposure and submergence were determined by fitting a polynomial on the pressure data and then extrapolating the time equivalent to a zero pressure. This value was used to calculate the length of time the tidal flat was exposed prior to the measurement of the critical shear stress.

Changes in mudflat elevation were determined using the ADV acoustic ping measurements. Both ADVs were firmly mounted on auger frames and remained at a constant elevation throughout the experiment. An acoustic ping measured the distance from the instrument to bed height at the beginning and end of each measurement period. The effective deposition during each tidal cycle was calculated as the difference between the maximum distance from the ADV (which represents the maximum erosion) and the final distance before exposure. Both the bed elevation and effective deposition during the previous immersion were considered as possible factors affecting daily changes in critical shear stress.

Chlorophyll a

Duplicate subcores were taken in each of the twelve experimental plots on alternate days for analysis of chlorophyll *a*. The subcores were 1 cm in diameter and sampled the top 1 cm of tidal flat sediment. Each was divided into 0.5 cm increments and frozen until analysis. For quantification of sediment chlorophyll *a* concentration, sediment subcore sections were thawed, sonicated, and extracted in 90% acetone overnight (Dalsgaard et al. 2000). Extracted samples were then centrifuged and 2 mL aliquots were analyzed for chlorophyll *a* fluorescence on a Turner Trilogy Fluorometer.

Sediment Characteristics

Syringe core samples were used to monitor changes in the density and organic content of each subplot. A 15 cc sediment sample was taken each day in conjunction with the critical shear stress measurements. The samples were dried in an oven at 60° C, and weighed to determine dry density. The samples were pulverized with a mortar and pestle, weighed and put into an oven at 200° C for 24 hours, and re-weighed to determine the percent organic material in the sample. Soil temperature was measured in each subplot daily during the sampling period using a Decagon 5 TM Water and Temperature Probe and ProCheck Handheld reader.

A 50cc sample was taken from each subplot on the first and last days of field observations. The samples were sieved to determine the percent of sand and silt/clay present at the study site and determine any variations in grain size of the sand across the

transect. The median grain size of sand was determined using the geometric method of moments in GRADISTATv8 (Blott and Pye 2001).

Meteorological Conditions

A weather station run by the Marine Biological Laboratory (MBL) at Marshview Field Station was used to monitor daily meteorological conditions (Figure 1). All data were collected using a Campbell Scientific CR10X data logger and averaged for 15 minutes. Air temperature and relative humidity were measured using a Vaisala HPM45C. Wind speed was measured using an RM Young 05103. Precipitation was recorded using Texas Electronic TE525WS-L. Solar radiation was measured using a Licor LI200X-L pyranometer. All sensors were mounted 3.048 m (10 feet) above ground level.

Evaporation Rates

Changes in daily meteorological conditions affect the rate of evaporation and therefore the soil characteristics of tidal flat sediments. The evaporation rate was calculated using the temperature of the sediments collected together with the critical shear stress and weather data at the time of tidal flat emersion. The evaporation rate was calculated using the mass transfer approach when the sediment temperature was available (i.e. tidal cycles when the critical shear stress was measured). The evaporation E reads (Dingman, 1994):

$$E = K_E v_a (e_{soil} - e_{air})$$

(1)

Where K_E is the efficiency of vertical water vapor transport, v_a is wind speed, and e_{soil} and e_{air} are the vapor pressures of the soil surface and air respectively. K_E is calculated as (Dingman, 1994):

$$K_E = \frac{D_{WV}}{D_M} \frac{0.622\rho_a}{P\rho_w} \frac{1}{6.25 \ln\left[\left(\frac{z_m - z_d}{z_0}\right)\right]^2}$$

(2)

Where D_{WV} is the diffusivity of water vapor D_M is the diffusivity of momentum, z_o is the roughness height, z_d is the zero-plane displacement, z_m is the elevation at which wind speed is measured, P is the atmospheric pressure, ρ_a and ρ_w the densities of air and water respectively.

The vapor pressure of air and soil are (Dingman, 1994):

$$e_{air} = 6.11 \, W_a \exp\left(\frac{17.3T_{air}}{T_{air} + 237.2}\right)$$

$$e_{soil} = 6.11 \, \exp\left(\frac{17.3T_{soil}}{T_{soil} + 237.2}\right)$$

(3)

Where W_a is the relative humidity, T_{air} and T_{soil} are the temperature of the air and soil in °C.

Penman's equation was used to estimate the evaporation rate when soil temperature data were absent (i.e. when critical shear stress measurements were not taken). According to this equation, the rate of evaporation is calculated as (Dingman, 1994):

$$E = \frac{s(T_a)(K + L) + \Upsilon\rho\lambda_v K_E v_a e_{sat}(T_a)(1 - W_a)}{\rho\lambda_v(s(T_a) + \Upsilon)}$$

Where K is solar radiation, L is net long wave radiation, v_a is wind speed, Υ is the psychometric constant, K_E is the efficiency of vertical water vapor transport, λ_v is the latent heat of vaporization, $s(T_{air})$ is the slope of saturation vapor pressure curve and $e_{sat}(T_{air})$ is the vapor pressure of air at saturation. K_E is calculated using Eq.2. Published constant values were used for the latent heat of vaporization (2257 kJ/kg), the psychometric constant (.66 mbar/C) and density of water (1000 kg/m^3). $s(T_{air})$ and $e_{sat}(T_{air})$ are calculated as (Dingman, 1994):

$$s(T_{air}) = \frac{25083}{(T_{air} + 237.3)^2} \exp\left(\frac{17.3\, T_{air}}{T_{air} + 237.3}\right)$$

(5)

$$e_{sat}(T_{air}) = 6.11 \exp\left(\frac{17.3\, T_{air}}{T_{air} + 237.3}\right)$$

(6)

Net long wave radiation is calculated as the difference between incoming atmospheric radiation (L_{at}) and radiation emitted by the sediment surface (L_w). L is calculated as (Abramowitz et al., 2012; Dingman, 1994):

$$L = L_{at} - L_w$$

$$L_{at} = (.031 e_{air} + 2.84\, T_{air} - 522.5) * .001$$

$$L_w = \varepsilon_w \sigma\, (T_{air} + 273.15)^4$$

(7)

Published constant values were used for the emissivity of water, ε_w (0.97) and the Stefan-Boltzmann constant (5.67*10^{-11} KW / (m^{2}K^4).

In order to calculate the efficiency of vertical water vapor transport, K_E, for both versions of the evaporation equation, an acceptable roughness height, z_0, had to be determined for the study site. This was computed by comparing the rate of evaporation calculated on each day using both methods. A value of $z_0=.158$ m was found by minimizing the mean squared error between the two values.

The evaporation rate was multiplied by the length of exposure to determine the evaporation that occurred prior to the critical shear stress measurement. Exposure time was determined by the ADV1 pressure data; time of critical shear strength measurements was taken from the CSM measurement timestamp. Total evaporation during emersion was instead defined as evaporation rate times the total period of tidal emersion. Exposure and submergence time were determined by the ADV1 pressure data.

Statistical Analysis

A multi-faceted approach was used for the statistical analysis of the field observations component of this study. The differences between critical shear stress measurements in the nutrient-enriched and control transects and between measurements taken in the same subplot of each transect on different days were tested using a two-way ANOVA. The influence that each measured factor (chlorophyll *a*, sediment characteristics, and meteorological conditions) had on the critical shear stress was determined through a correlation analysis. The combined influence of all variables reporting a significant correlation with critical shear stress was determined through a multiple regression analysis.

The influence the maximum shear stress exerted on tidal flat sediments and total evaporation over emersion periods exerted individually on the maximum ADV backscatter during the following flood period was analyzed using correlation analysis. A multiple regression analysis was used to determine how much of the variability seen in the maximum ADV backscatter can be accounted for by considering both of these factors together.

The Cook's Distance approach was used to identify outliers before each analysis was conducted. Any data point with a $D_i > 4/n$ was not considered.

Results

Sediment Characteristics

Sediment characteristics of both control and nutrient enriched transects remained relatively unchanged throughout the experiment. Average dry density fluctuated daily between 900-1100 g/m^3. No significant difference in dry density was found between the two plots. Although some fluctuations in the daily dry density were recorded, no trends were found in these fluctuations.

Percent organic material in the control and nutrient enriched plot showed no significant change between the two transects or over the duration of the experiment. The mean percent organic material varied daily from 3 to 4.5%; however, no long-term trends emerged from the data.

Finally, little variation in grain size was seen from samples taken at the beginning and end of the experimental period. Samples from each subplot at the beginning and end of

the experiment showed the sediments were approximately 60-65% clay / silt and 35-40% sand.

Effects of Nutrient Enrichment

A significant difference in the critical shear strength measured by the CSM was found between the nutrient enriched and control transects (p<.01). Sediments in the control transect consistently exhibited higher critical shear stress than those in the fertilized transect (Figure 3). No significant difference in chlorophyll *a*, dry density, organic content, and grain size was found between the two transects.

Additionally, a significant difference was found in the daily critical shear stress measurements taken within the same subplots on different days (p<.01), implying that variations in daily environmental conditions were affecting sediment erodability within the subplots. A two-way ANOVA analysis failed to conclude that differences within individual subplots are independent of the difference between the nutrient enriched and control transects (p=0.58), suggesting the same process may be responsible for both of these conclusions.

Factors Controlling Substrate Critical Shear Stresses

Correlation analysis showed that the length of exposure to air prior to the CSM measurement cannot explain the differences in critical shear stress (Table 1, Figure 4). In

fact, the variability in critical shear stress increased as sediments were exposed for a longer period of time (Figure 4).

When the daily evaporation rate was considered together with the length of exposure (total evaporation), a significant relationship with critical shear stress was found ($p<.01$) (Table 1, Figure 5a). The correlation coefficient improved considerably (from .27 to .45) when the control plot was considered by itself (Table 1).

A negative relationship existed between chlorophyll *a* and the critical shear strength of tidal flat sediments ($p=.01$) (Table 1, Figure 5b), indicating that microphytobenthos were fewer when the sediment was stronger. A weak relationship was found between chlorophyll *a* concentration and the total evaporation calculated prior to the CSM measurements ($p=.08$) (Fig. 5c). It should be noted that the time at which chlorophyll *a* samples were taken was not recorded and we used the time of the CSM measurements as a proxy. As a consequence the relationship between total evaporation and chlorophyll *a* may be stronger than depicted in this analysis.

The critical shear stress of tidal flat sediments was also found to be significantly correlated to the average bed elevation measured by the ADV ($p=.03$, Table 1).

A multiple regression analysis was used to determine which significant variables from the correlation analysis were collectively contributing to changes in the observed critical shear stress of the tidal flat sediments. Only combining the total evaporation and the average change in bottom elevation of all data points resulted in both factors remaining significant ($p<0.05$). However, the average change in bottom elevation was not significant when only the control plots were considered. Total evaporation and

21

chlorophyll *a* were not significantly correlated with critical shear stress when considered together in a multiple regression analysis, due to the existing relationship between these two variables (Figure 5c).

Factors Affecting Turbidity on the Rowley River Tidal Flats

Acoustic backscatter recorded by the ADVs during the flood period was used as a proxy for sediment resuspension occurring on the tidal flat as well as for sediments remobilized in the entire Plum Island Sound and then funneled in the Rowley River.

Maximum shear stress exerted locally on the tidal flat during flood explained approximately 40% of the variability in backscatter recorded by the ADV (p<.01) (Figure 6a). Total evaporation was also statistically correlated to the maximum acoustic backscatter (p=.015) recorded during the subsequent tidal cycle, and explained approximately 21% of the variability (Figure 6b). A multiple regression analysis showed that the total evaporation occurring during the previous tidal cycle and the maximum shear stresses exerted on the tidal flat during flood are independent factors, both controlling the maximum acoustic backscatter and therefore sediment resuspension. Both factors remain statistically significant when considered together and explained approximately 54% of the variability in maximum backscatter (p<.01, p=.035).

Discussion

The results of this study show that evaporation controls daily variations in sediment erodability in tidal flat sediments. The critical shear stress of the substrate increases as evaporation occurs over the emersion period.

Critical shear stress measurements were taken in the nutrient enriched transect prior to the control transect as part of the measurement procedure. Therefore, evaporation had a longer period of time to desiccate and strengthen the sediments prior to measurement. This procedural bias offers an explanation for the significantly lower critical shear stress observed in the fertilized transect throughout the study.

The extent of evaporation tidal flat sediments undergo depends on meteorological conditions (temperature, relative humidity, wind conditions, and solar radiation) as well as the duration of exposure to air. As these conditions change between emersion periods, so does the rate of evaporation and therefore the critical shear stress of the tidal flat sediments. Days with strong winds, warmer temperatures or more sunlight favor higher evaporation rates. As sediments are exposed for longer lengths of time, these differences become more pronounced, leading to the increased variability in sediment critical shear stress (Figure 4).

For example, significant variations in the average critical shear stress were evident between September 12 and September 15 (Figure 3). The rate of evaporation during emersion increased each day from September 12 to September 14 due to progressively earlier sunrises in relation to the tidal cycle and higher air temperature during emersion (Figure 7). Additionally, September 14 exhibited high wind speeds and low relative

humidity at the beginning of the emersion period before critical shear stress measurements were taken. Although sunrise occurred earlier in the tidal cycle on September 15 than on September 14, the solar radiation was less intense, air temperature was similar, while wind speed was low and relative humidity high. These conditions led to a decrease in the rate of evaporation and therefore a decrease in the critical shear stress measured on September 15 (Figure 3). This evidence supports our finding that the critical shear stress of tidal flat measurements varies significantly with meteorological conditions they are exposed to during emersion. Varying meteorological conditions must be considered to correctly interpret changes in critical shear strength in studies spanning multiple days, and particularly across months or seasons.

A significant correlation between evaporation and the critical shear stress exists when all data are considered; however, the correlation increased considerably when measurements taken in the control transect are considered alone (R^2 improves from .27 to .45). This is likely due to the addition of water during the nutrient enrichment process partially offsetting the desiccation that had previously occurred. The application of nutrients and water likely had a similar effect on sediment as rain, which has been shown to return the critical shear stress of sediments to levels similar to those just after emersion (Tolhurst et al, 2005).

Although a significant difference in the critical shear stress measurements taken between the nutrient enriched and control transects was observed, no significant difference was found in the chlorophyll a concentrations. This result implies that the nutrient enrichment did not have an effect on the microphytobenthos community at the

concentration and frequency applied in this experiment. The most likely explanation for this surprising result is that a higher concentration of fertilizer or a longer period of time at the same concentration may have been required to see a significant change in chlorophyll *a* concentration. For example, the fertilizer may have been washed away after few hours when the incoming tide flooded the mudflat, minimizing its impact on the microphytobenthos community. Alternatively, a higher concentration of fertilizer or a longer period of time at the same concentration may have been required to see a significant change in chlorophyll *a* concentration.

Previous studies have shown that biofilm abundance, measured using chlorophyll *a* as a proxy, has a positive effect on the critical shear strength of tidal flat sediments (Tolhurst, 2008, Defew, 2002). On the contrary, our study found a negative relationship between these two variables. Diatoms, which are dominant in microphytobenthos, are known to migrate into the sediment over the tidal cycle as water content decreases (Coelho, 2009). Therefore the decrease in chlorophyll *a* may be a result of diatom migration due to sediment desiccation rather than a direct effect of biofilms on critical shear stress. If this is true, the relationship between chlorophyll *a* concentration and critical shear stress may not be causal but just reflect the relationship found between total evaporation and critical shear stress.

In addition to the total evaporation and chlorophyll *a* measurements, the average elevation of the mudflat during the previous immersion period was significantly correlated to the critical shear stress. Changes in bed height are a result of erosion and deposition that occurred during the previous immersion cycle. A lower elevation implies

an erosion event and the re-exhumation of more compact and resistant sediments. A higher elevation indicates a deposition event, with soft sediment accumulated at the surface. Although changes in the average bed height during the preceding immersion period showed statistical significance with the critical shear stress of sediments, a low correlation coefficient (R^2=.06) indicates that this interaction was limited.

It is important to note that tidal flats are subject to erosion and deposition only during immersion periods. Therefore, the importance of our findings from data taken during emersion periods is limited unless the substrate retains its strength after flooding.

The maximum shear stress exerted on the tidal flat by currents occurs during flood, approximately 1-1.5 hours after submergence, and varies with tidal amplitude (larger tides trigger larger shear stresses, Figure 2). Higher measured shear stresses translate to increased sediment resuspension, leading to a relationship between measured shear stresses and acoustic backscatter (a proxy for sediment concentration) during flood.

The influence of shear stress on the maximum acoustic backscatter was easily observed towards the end of the study period when spring tides were creating strong flood currents (Figure 2). In fact, from September 23 to September 28, as the tidal range became larger, the shear stress exerted on the tidal flat sediments increased. Accordingly, the acoustic backscatter signal generally grew across this period. However, careful examination shows that current shear stress alone cannot be responsible for all of the variability in acoustic backscatter among tidal cycles. In fact, the acoustic backscatter should follow the variations in maximum shear stress between the evening of September 23 and the morning of September 24 and between the two tidal cycles on September 26. In each of

these examples, a noticeable increase in the shear stress exerted on the tidal flat

sediments does not correspond to an increase in the acoustic backscatter signal.

Therefore, additional factors must have an influence on the rate of sediment resuspension

on the tidal flat during the flood period.

In addition to the positive correlation with shear stress, the rate of sediment

resuspension during flood is negatively related to the amount of evaporation during the

previous tidal cycle (p =.015) This finding proves evaporation affects sediment

erodability not only during emersion, but also during the following immersion period

(Figure 6b).

While other sediment properties such as density, organic content, grain size, and

fraction of clay and silt, may have a significant effect on substrate strength at varying

locations within the estuary, these factors were not found to vary at our site.

Energetic events in the sound (i.e. storms) and evaporation are not independent

processes. Increased cloud cover and rainfall during storms reduce evaporation during

low tide. Therefore, a bimodal configuration is likely to exist wherein long periods of

fair weather reduce sediment resuspension by the compound effect of dessication and

limited hydrodynamic energy. On the other hand, storms lasting for several tidal cycles

have a double effect on sediment remobilization, with wet conditions during low tide

softening the sediments that are then eroded during high tide.

Evaporation processes should be more important in environments with large intertidal

areas exposed at low tide. Higher tidal oscillations expose large intertidal areas at low

tide in meso and macrotidal environments (e.g. Fagherazzi et al. 2007, Fagherazzi and Wiberg 2009), such as the study area presented here.

Seasonal variability in meteorological conditions should also affect mudflat erosion and sediment resuspension. Summer months favor desiccation thus reducing erodability, while cold winter months increase potential erosion. Global warming might therefore decrease the erodability of intertidal areas by promoting desiccation during emersion.

Conclusions

A study conducted on a tidal flat in Plum Island Sound, Massachusetts to determine factors contributing to variability in sediment erodability found that:

1) Nutrient enrichment of tidal flat sediments with 70 μM NO_3^- for two weeks does not trigger an increase of chlorophyll a in the sediments nor an increase in sediment critical shear stress, indicating that the microphytobenthos community remains unaffected.

2) The critical shear stress of tidal flat sediments increases over the emersion period. The critical shear stress increases faster on days with high evaporation rates and slowly on days with low evaporation rates.

3) Chlorophyll a, a proxy for microphytobenthos, decreases over the emersion period as the total evaporation increases.

4) Variability in the suspended sediment concentration during the flood period of the tidal cycle may be explained by the evaporation occurring in the emersion period prior to the flood as well as the critical shear stress exerted on the sediment.

Bibliography

Amos, C. L., Daborn, G. R., Christian, H. A., Atkinson, A., & Robertson, A. 1992. In situ erosion measurements on fine-grained sediments from the Bay of Fundy. Marine Geology, 108(2), 175-196.

Andersen, T. J., Fredsoe, J., & Pejrup, M. 2007. In situ estimation of erosion and deposition thresholds by Acoustic Doppler Velocimeter (ADV). Estuarine, Coastal and Shelf Science, 75(3), 327-336.

Baeshad, I. 1955. Absorptive and swelling properties of clay-water system. Bulletin, (169), 70.

Black, K. S., Tolhurst, T. J., Paterson, D. M., & Hagerthey, S. E. 2002. Working with natural cohesive sediments. Journal of Hydraulic Engineering, 128(1), 2-8.

Blott, S. J., & Pye, K. 2001. GRADISTAT: a grain size distribution and statistics package for the analysis of unconsolidated sediments. Earth surface processes and Landforms, 26(11), 1237-1248.

Carr, J., D'Odorico, P., McGlathery, K., & Wiberg, P. 2010. Stability and bistability of seagrass ecosystems in shallow coastal lagoons: Role of feedbacks with sediment resuspension and light attenuation. Journal of Geophysical Research, 115(G3), G03011.

Chanson, H., Takeuchi, M., & Trevethan, M. 2008. Using turbidity and acoustic backscatter intensity as surrogate measures of suspended sediment concentration in a small subtropical estuary. Journal of environmental management, 88(4), 1406-1416.

Coelho, H., Vieira, S., & Serôdio, J. 2009. Effects of desiccation on the photosynthetic activity of intertidal microphytobenthos biofilms as studied by optical methods. Journal of Experimental Marine Biology and Ecology, 381(2), 98-104.

Commonwealth of Massachusetts. Executive Office of Environmental Affairs, Massachusetts Watershed Initiative 2003. Parker River Low Flow Study. http://www.businessevision.info/parker_river/ ParkerRiverLowStudyFinalReport.pdf. August, 2012.

Commonwealth of Massachusetts.Executive Office of Environmental Affairs, Massachusetts Department of Environmental Protection, Bureau of Resource Protection, Division of Watershed Management. 1999. Parker River Watershed Water Quality Assessment Report. http://www.mass.gov/dep/water/resources/91wqar99.pdf. August, 2012.

Dalsgaard, T. (ed.), Nielsen, L.P., Brotas, V., Viaroli, P., Underwood, G., Nedwell, D. B., Sundbäck, K., Rysgaard, S., Miles, A., Bartoli, M., Dong, L., Thornton, D.C.O., Ottosen, L.D.M., Castaldelli, G. &Risgaard-Petersen, N. 2000: Protocol handbook for NICE - Nitrogen Cycling in Estuaries: a project under the EU research programme: Marine Science and Technology (MAST III). National Environmental Research Institute, Silkeborg, Denmark.62 pp.

Davoult, D., Migné, A., Créach, A., Gévaert, F., Hubas, C., Spilmont, N., & Boucher, G. 2009. Spatio-temporal variability of intertidal benthic primary production and respiration in the western part of the Mont Saint-Michel Bay (Western English Channel, France). Hydrobiologia, 620(1), 163-172.

Defew, E. C., Tolhurst, T. J., & Paterson, D. M. 2002. Site-specific features influence sediment stability of intertidal flats. Hydrology and Earth System Sciences Discussions, 6(6), 971-982.

Fagherazzi S., FitzGerald D.M., Fulweiler R.W., Hughes Z., Wiberg P.L., McGlathery K.J., Morris J.T., Tolhurst T.J., Deegan L.A., Johnson D.S. 2012. Ecogeomorphology of Salt Marshes, Treatise on Geochemistry, Volume 12. Ecogeomorphology. Editors: Butler D., Hupp C., Executive Editor: Shroder J. Elsevier.

Fagherazzi, S., & Wiberg, P. L. 2009. Importance of wind conditions, fetch, and water levels on wave-generated shear stresses in shallow intertidal basins. Journal of Geophysical Research, 114(F3), F03022.

Fagherazzi, S., & Mariotti, G. 2012. Mudflat runnels: Evidence and importance of very shallow flows in intertidal morphodynamics. Geophysical Research Letters, 39(14), L14402.

Fagherazzi, S., Palermo, C., Rulli, M. C., Carniello, L., & Defina, A. (2007). Wind waves in shallow microtidal basins and the dynamic equilibrium of tidal flats. Journal of geophysical research, 112(F2), F02024.

Fugate, D. C., & Friedrichs, C. T. 2003. Controls on suspended aggregate size in partially mixed estuaries. Estuarine, Coastal and Shelf Science, 58(2), 389-404.

Galbraith, H., Jones, R., Park, R., Clough, J., Herrod-Julius, S., Harrington, B., & Page, G. 2002. Global climate change and sea level rise: potential losses of intertidal habitat for shorebirds. Waterbirds, 25(2), 173-183.

Hillel, D. 1998. Environmental soil physics: Fundamentals, applications, and environmental considerations. Academic press.

Kim, S. C., Friedrichs, C. T., Maa, J. Y., & Wright, L. D. 2000. Estimating bottom stress in tidal boundary layer from acoustic Doppler velocimeter data. Journal of Hydraulic Engineering, 126(6), 399-406.

Lawson, S. E., Wiberg, P. L., McGlathery, K. J., & Fugate, D. C. 2007. Wind-driven sediment suspension controls light availability in a shallow coastal lagoon. Estuaries and coasts, 30(1), 102-112.

Little, C. 2000. The biology of soft shores and estuaries. Oxford University Press, USA.

Lohrmann, A. 2001. Monitoring sediment concentration with acoustic backscattering instruments. Nortek Technical Note, (003), 9.

Mariotti, G., Fagherazzi, S., Wiberg, P. L., McGlathery, K. J., Carniello, L., & Defina, A. 2010. Influence of storm surges and sea level on shallow tidal basin erosive processes. Journal of Geophysical Research, 115(C11), C11012.

Mariotti, G., & Fagherazzi, S. 2012. Wind waves on a mudflat: the influence of fetch and depth on bed shear stresses. Continental Shelf Research.

Meire, P., Ysebaert, T., Damme, S. V., Bergh, E. V. D., Maris, T., & Struyf, E. 2005. The Scheldt estuary: a description of a changing ecosystem. Hydrobiologia, 540(1), 1-11.

Miller, D. C., Geider, R. J., & MacIntyre, H. L. 1996. Microphytobenthos: the ecological role of the "secret garden" of unvegetated, shallow-water marine habitats. II. Role in sediment stability and shallow-water food webs. Estuaries and Coasts, 19(2), 202-212.

Paterson, D. M. 1989. Short-term changes in the erodibility of intertidal cohesive sediments related to the migratory behavior of epipelic diatoms. Limnology and Oceanography, 223-234.

Pusch, R., & Yong, R. 2003. Water saturation and retention of hydrophilic clay buffer—microstructural aspects. Applied clay science, 23(1), 61-68.

Rider, N. E., & Rider, N. E. 1954. Eddy diffusion of momentum, water vapour, and heat near the ground. Philosophical Transactions of the Royal Society of London. Series A, Mathematical and Physical Sciences, 246(918), 481-501.

Scavia, D., Field, J. C., Boesch, D. F., Buddemeier, R. W., Burkett, V., Cayan, D. R., ... & Titus, J. G. 2002. Climate change impacts on US coastal and marine ecosystems. Estuaries and Coasts, 25(2), 149-164.

Tobias, C., Giblin, A., McClelland, J., Tucker, J., & Peterson, B. (2003). Sediment DIN fluxes and preferential recycling of benthic microalgal nitrogen in a shallow macrotidal estuary. Marine ecology. Progress series, 257, 25-36.

Tolhurst, T. J., Black, K. S., Shayler, S. A., Mather, S., Black, I., Baker, K., & Paterson, D. M. 1999. Measuring the in situ Erosion Shear Stress of Intertidal Sediments with the Cohesive Strength Meter (CSM). Estuarine, Coastal and Shelf Science, 49(2), 281-294.

Tolhurst, T. J., Jesus, B., Brotas, V., & Paterson, D. M. 2003. Diatom migration and sediment armouring–an example from the Tagus Estuary, Portugal. Hydrobiologia, 503(1), 183-193.

Tolhurst, T. J., Defew, E. C., De Brouwer, J. F. C., Wolfstein, K., Stal, L. J., & Paterson, D. M. 2006. Small-scale temporal and spatial variability in the erosion threshold and properties of cohesive intertidal sediments. Continental shelf research, 26(3), 351-362.

Tolhurst, T. J., Defew, E. C., Perkins, R. G., Sharples, A., & Paterson, D. M. 2006. The effects of tidally-driven temporal variation on measuring intertidal cohesive sediment erosion threshold. Aquatic Ecology, 40(4), 521-531.

Underwood, G. J., & Paterson, D. M. 1993. Seasonal changes in diatom biomass, sediment stability and biogenic stabilization in the Severn Estuary. Journal of the Marine Biological Association of the United Kingdom, 73(04), 871-887.

Van Damme, S., Struyf, E., Maris, T., Ysebaert, T., Dehairs, F., Tackx, M., ... & Meire, P. 2005. Spatial and temporal patterns of water quality along the estuarine salinity gradient of the Scheldt estuary (Belgium and The Netherlands): results of an integrated monitoring approach. Hydrobiologia, 540(1), 29-45.

Widdows, J., Friend, P. L., Bale, A. J., Brinsley, M. D., Pope, N. D., & Thompson, C. E. L. 2007. Inter-comparison between five devices for determining erodability of intertidal sediments. Continental shelf research, 27(8), 1174-1189.

Zhan, T. L., & Ng, C. W. (2006). Shear strength characteristics of an unsaturated expansive clay. Canadian Geotechnical Journal, 43(7), 751-763.

Vita

Appendix 1: Tables

	R^2	B	P
Average Distance	0.0626	+	0.0282
Chlorophyll a	0.3215	-	0.0113
Density	0.0001	-	0.9291
Deposition	0.007	-	0.4692
Evaporation - All	0.27	+	0.000153
Evaporation - Control Only	0.4455	+	0.000366
Length of Exposure	0.0196	+	0.225
Final Distance	0.0274	+	0.1501
Maximum Shear Stress	0.0195	-	0.2254
Organic Content	0.0209	-	0.2224
PAR	0.00018	-	0.9076

Table 1: Results of Correlation Analysis between listed variables and critical shear strength of sediments. B represents the sign of the relationship between the listed variable and critical shear stress. Average Distance indicates the averaged distance from the ADV sensor head to bed over the previous tidal cycle. Highlighted lines represent significant relationships.

Appendix 2: Figures

Figure 1: Map of Plum Island Estuary including study site and Marshview weather station

Figure 2: Map of study site transects and ADV placement
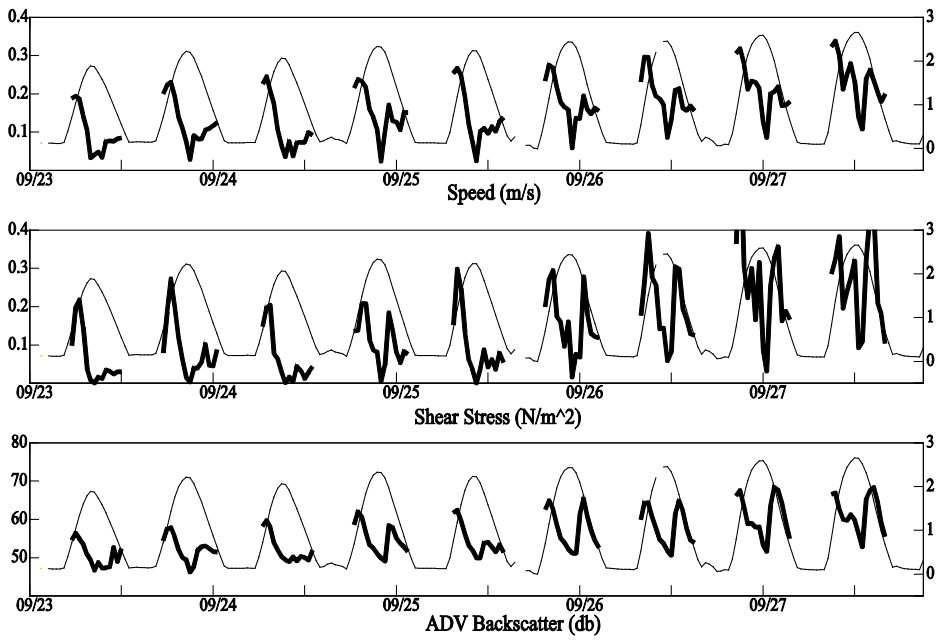
Figure 3: ADV Measurement Profile
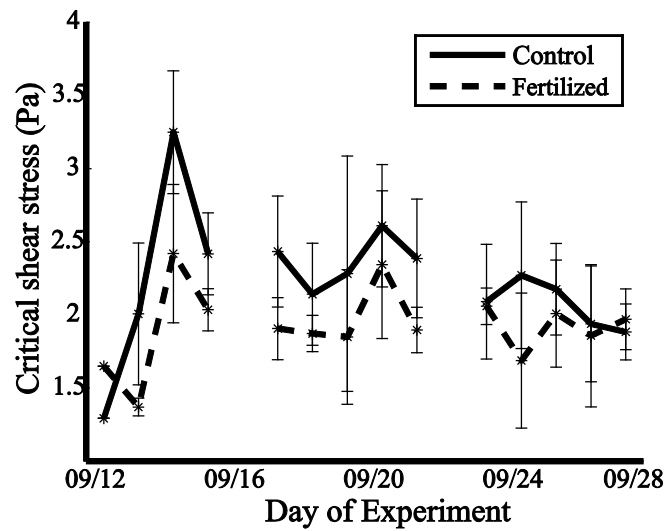
Figure 4: Mean Critical Shear Stress for Control and Fertilized Plots.

Solid line represents change in mean critical shear stress for control transect. Dashed line represents change in mean critical shear stress for nutrient enriched plot. Gray error bars are standard deviation.
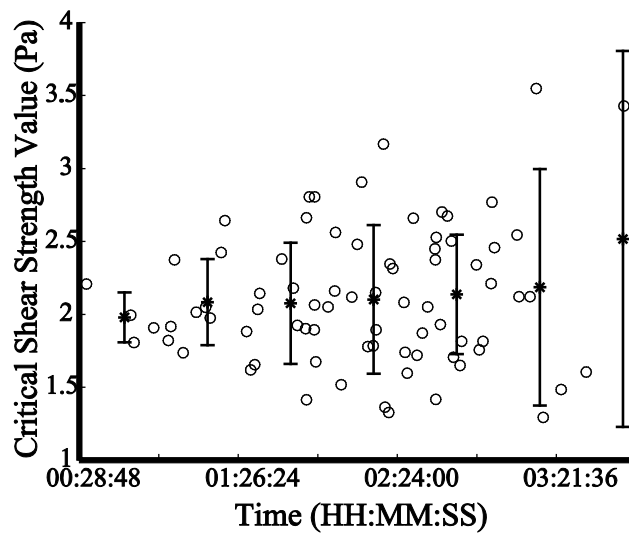
Figure 5: Critical Shear Stress versus Length of Exposure

Stars represent mean critical shear stress in 30 minute bins; line represents mean standard deviation within bins.
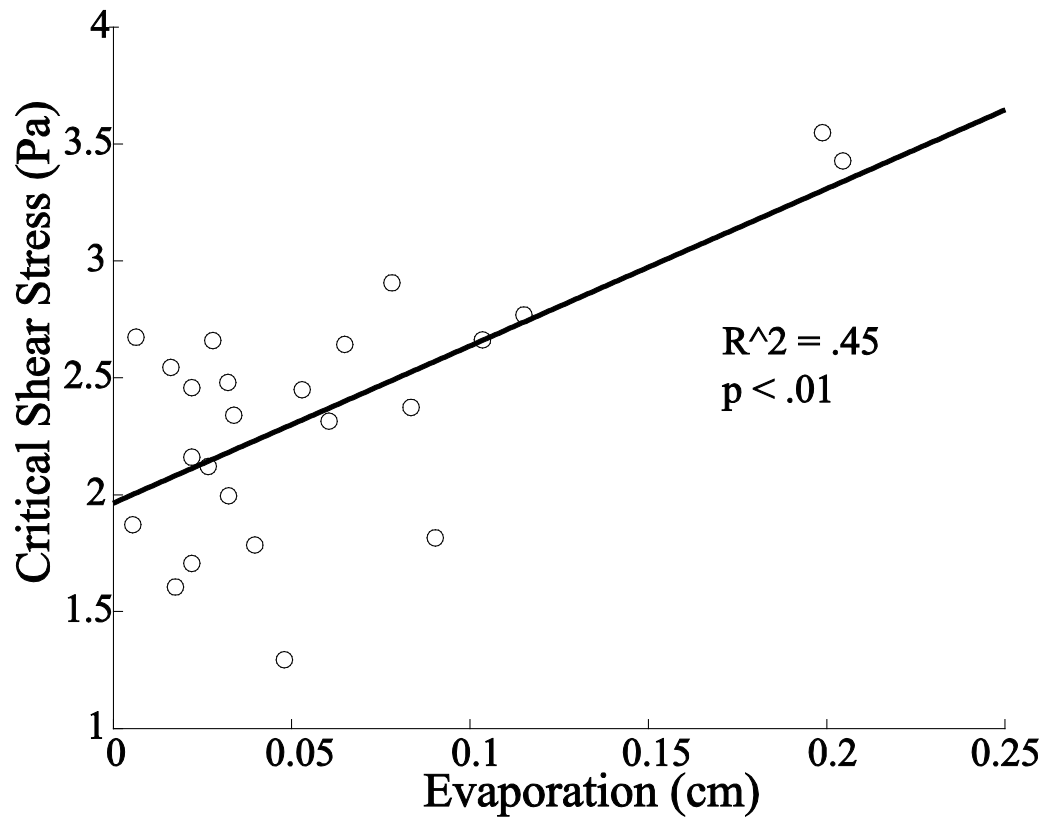
Figure 6: Correlation between Critical Shear Stress and Evaporation
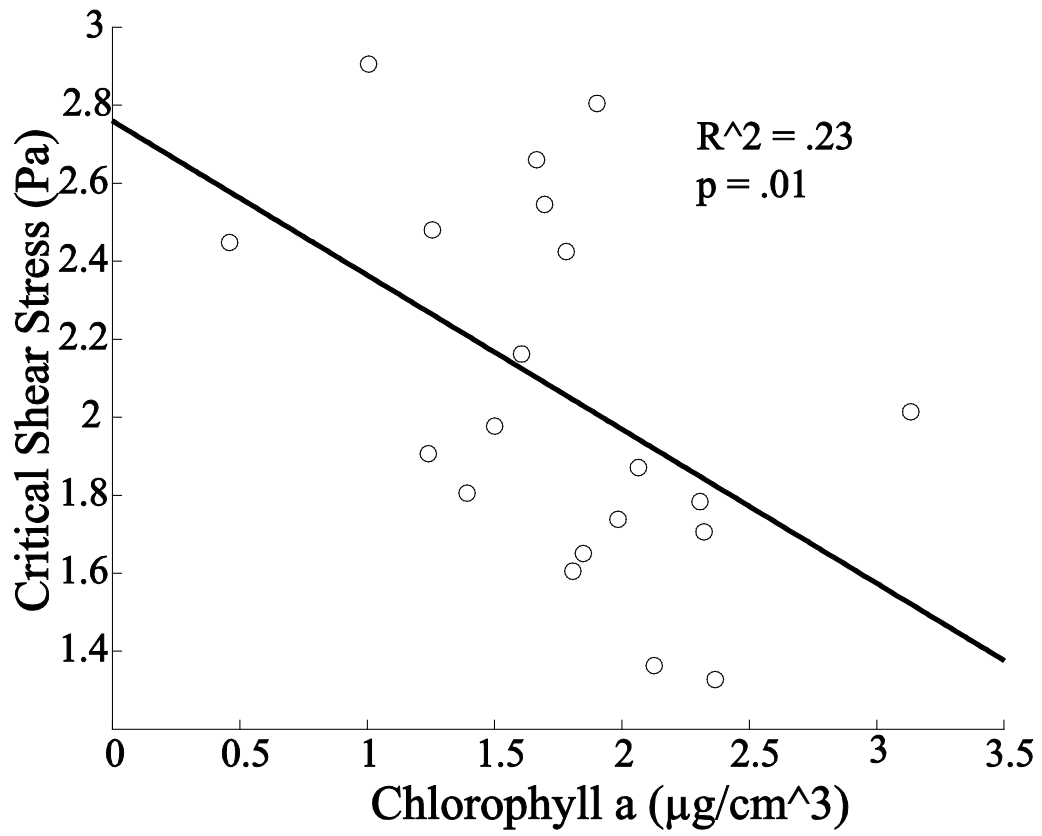
Figure 7: Correlation between Critical Shear Stress and Chlorophyll *a*
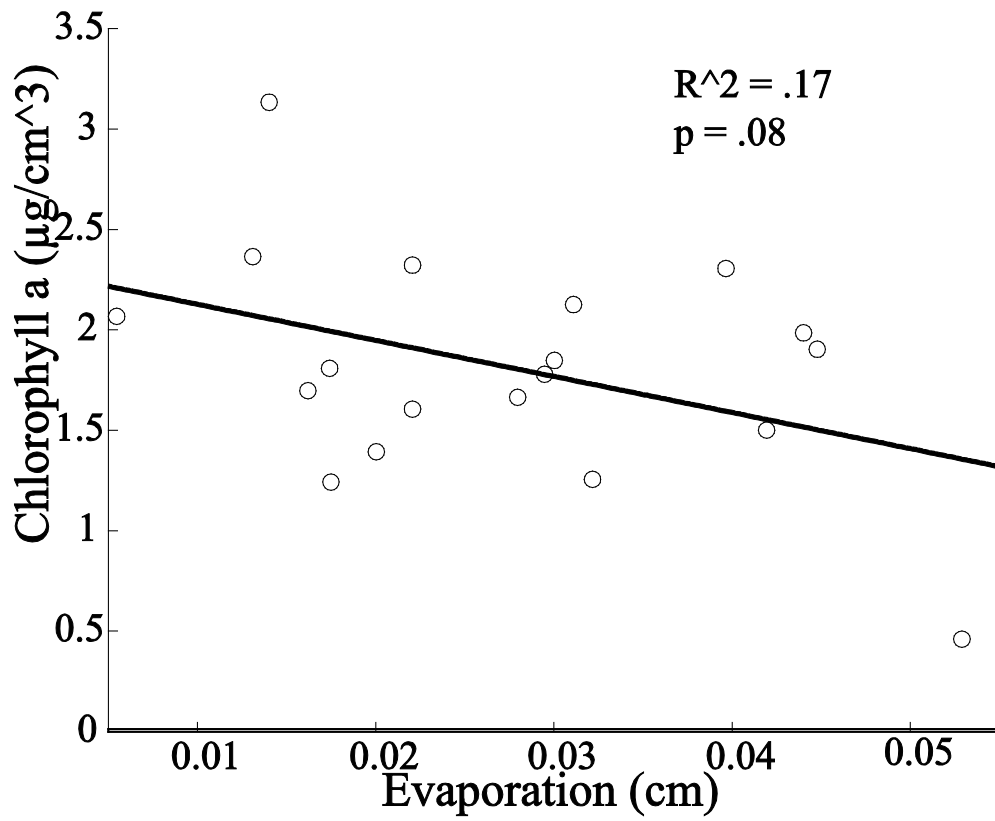
**Figure 8:** Correlation between Chlorophyll *a* and Evaporation
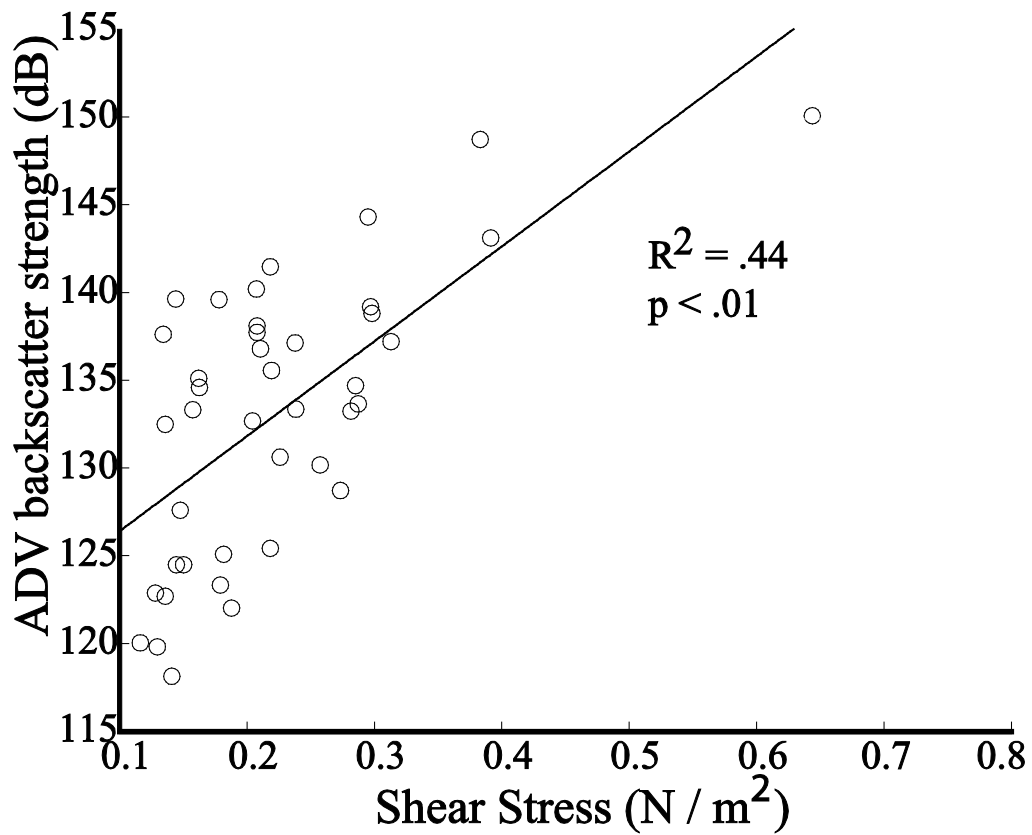
**Figure 9:** Shear Stress versus Maximum Backscatter
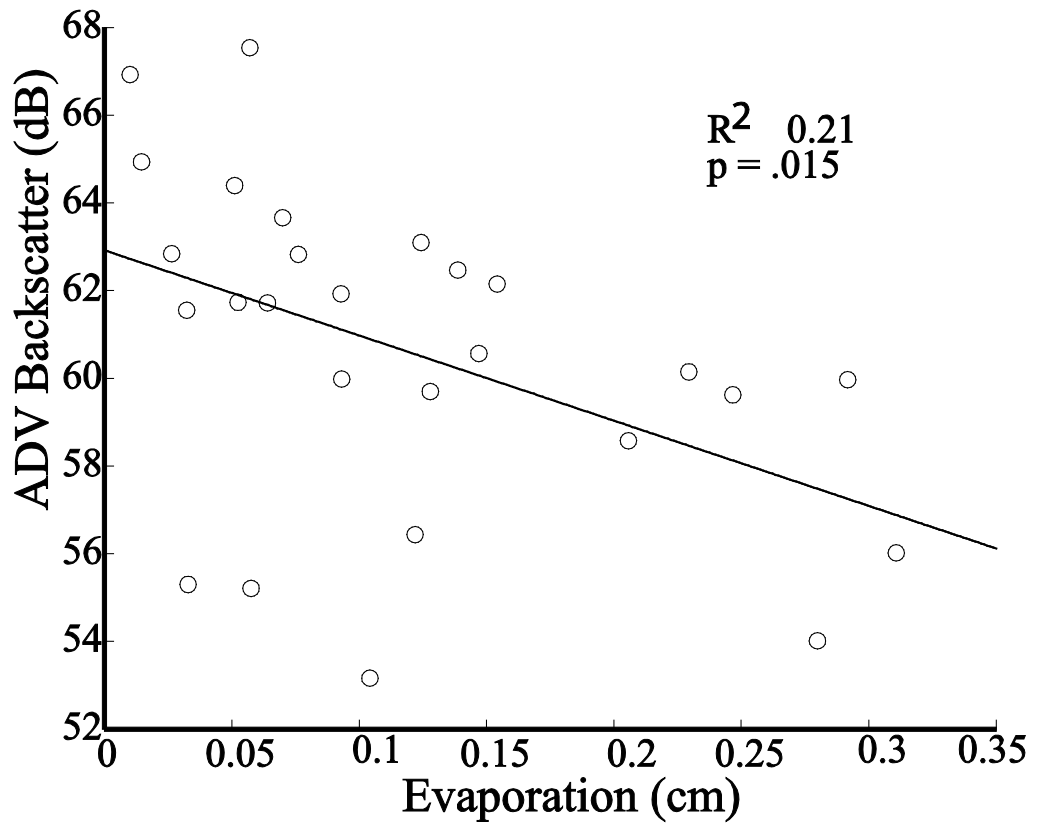
**Figure 10:** Evaporation versus Maximum Backscatter
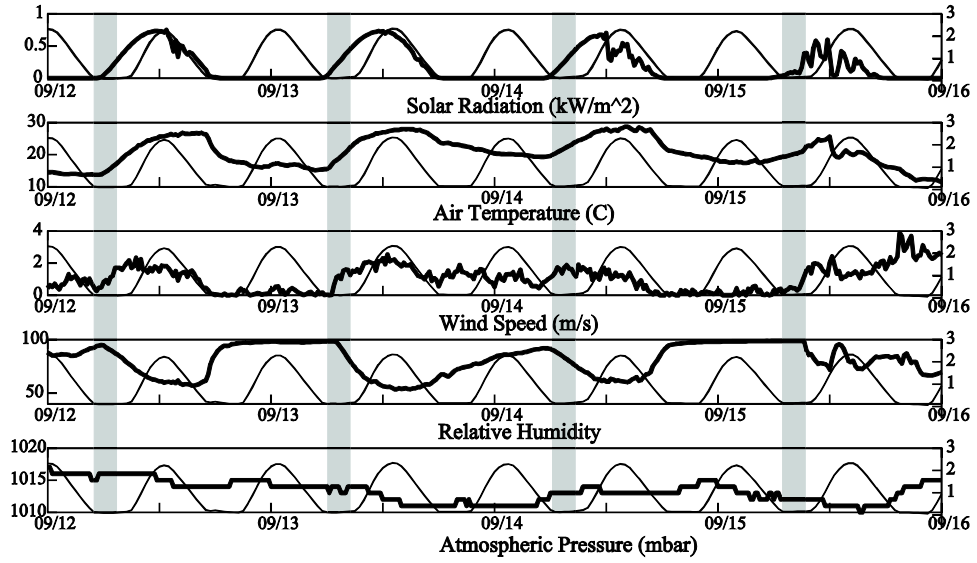
Figure 11: Meteorological Data from Marshview Field Station and ADV pressure data